

# Vector-borne diseases identification and quantification vectored by mosquitoes using the QIAcuity® Digital PCR System and qPCR

Laima Antanaviciute<sup>1</sup>, Athena Lemon<sup>2</sup>, Rachel Wofford<sup>2</sup>, Bi Linton<sup>1</sup>, Abelardo Moncayo<sup>2</sup>

<sup>1</sup> QIAGEN, 19300 Germantown Road, Germantown, MD 20874

<sup>2</sup> Tennessee Department of Health, 630 Hart Lane, Nashville TN 37216

## Introduction

Over 80% of the global population is threatened by vector-borne diseases (VBD), which cause significant global morbidity and mortality. VBD are caused by pathogens such as bacteria, parasites, or viruses transmitted via an arthropod vector. There has been a global increase in VBD as vector populations such as mosquitoes are increasing in population, range, and longevity (1-3). The increase in VBD can be attributed to environmental changes and the pervasiveness of insecticide resistance (1,2). Insecticide-based control approaches are becoming more ineffective due to the high-level resistance of these chemicals among arthropod populations. Therefore, it is crucial to establish and maintain VBD surveillance and control programs to reduce transmission and to prevent outbreaks.

Two commonly monitored mosquito-borne viruses are West Nile virus (WNV) and Flanders virus (FLAV). WNV is the leading cause of mosquito-borne disease in the continental United States. FLAV, also known to associate with mosquitos, has been shown to co-occur with WNV and thus is often used as a sentinel for WNV, with detection triggering public health control and prevention interventions.

The QIAcuity digital PCR (dPCR) system enables more sensitive detection of ultra-low concentration viral templates and eliminates the need for reference materials. For these reasons, digital PCR (dPCR) was used to detect

and quantify high and low concentration viruses vectored by mosquitoes that carry WNV and FLAV in a side-by-side comparison with quantitative real-time PCR (qPCR). The dPCR data generated by the QIAcuity instrument was compared to qPCR data as a means to assess sensitivity, reproducibility, and multiplexing capabilities. For this study, mosquitoes were collected from different locations across the state of Tennessee as part of the Tennessee Vector-Borne Diseases (VBD) surveillance and vector control.

## Materials and Methods

Mosquitoes were collected via stationary gravid trap in Memphis (Shelby County) and Nashville (Davidson County), Tennessee following previous published protocols (4). Adult *Culex pipiens* and *Culex quinquefasciatus* mosquitoes were sorted into pools of up to 50 mosquitoes according to date and trap site. *Cx. pipiens* and *Cx. quinquefasciatus* were pooled, as they are difficult to distinguish and are both vectors for WNV and FLAV. Samples were then labeled, stored, and shipped weekly at 4°C to the Tennessee VBD Laboratory. Fifty or fewer mosquitos were homogenized in a single tube following a previously published protocol in preparation for nucleic acid extraction (4). A QIAamp Virus BioRobot MDx extraction kit (Cat. No. 965652) ►

was used to extract RNA from mosquito samples following the manufacturer's instructions on a QIAGEN BioRobot Universal System. Samples were then used for downstream qPCR or dPCR applications.

For the first dPCR and qPCR comparison study, two samples that had produced high C<sub>T</sub> values (C<sub>T</sub>>30) and two samples that had produced low C<sub>T</sub> values (C<sub>T</sub><22) in a previous study were selected for analysis by qPCR and dPCR. For this analysis, single-plex reactions were set-up targeting the WNV target only.

For the second comparison study, three mosquito samples that were previously shown to be positive for both WNV and FLAV were selected for analysis by qPCR and dPCR. Samples were analyzed by both technologies in multiplex assays targeting both WNV and FLAV. Sample information for all six samples used in both comparison studies are presented in Table 1.

Non-diluted extracted RNA was analyzed in via qPCR using as described in Table 2 using WNV and FLAV assays reported in the literature (4-5). Average C<sub>T</sub> values were calculated for each sample.

For dPCR analysis, RNA samples extracted from the Samples 1-7 were diluted using DNase-free water (QIAGEN). For single-plex assays, stock,10-1, and 10-2 dilutions were used, whereas samples were diluted to 10-1,10-2, and 10-3 for the multiplex reactions. The QIAcuity One-Step Viral RT-PCR Kit (Cat.No. 1123145) was used to perform reverse transcription and PCR amplification of stock and diluted RNA samples following the manufacturer's protocol (QIAGEN, Germany). The samples were set-up in a duplex reaction amplifying the WNV and FLAV targets using two published sets of qPCR primer pairs and two different fluorophores corresponding to each target of interest (4, 5). The WNV assay used a hydrolysis probe labeled with a FAM fluorophore, whereas the FLAV assay used a hydrolysis probe labeled with a HEX fluorophore.

Reactions were first pre-mixed in 0.65 ml Eppendorf tubes, then 40 µl of the final reaction volume was transferred to a QIAcuity 26k 24-well Nanoplate (Cat.No. 250001). Single-plex and multiplex reaction assay set-up for use with the QIAcuity dPCR instrument is presented in Table 3.

**Table 1. Summary of mosquito samples collected and used in this study**

Comparison Study 1: Single-plex Reaction					
Mosquito sample	Number of mosquitoes per sample	Assay	Approximate WNV C <sub>T</sub> value	Approximate FLAV C <sub>T</sub> value	Location
Sample 1	50	WNV	Not Detected	N/A	Shelby County, TN
Sample 2	33	WNV	~32	N/A	Shelby County, TN
Sample 3	50	WNV	~22	N/A	Shelby County, TN
Sample 4	19	WNV	~22	N/A	Davidson County, TN

**Comparison Study 2: Multiplex Reaction**

Mosquito sample	Number of mosquitoes per sample	Assay	Approximate WNV C <sub>T</sub> value	Approximate FLAV C <sub>T</sub> value	Location
Sample 5	50	WNV/FLAV	~25	~20	Shelby County, TN
Sample 6	50	WNV/FLAV	~26	~18	Shelby County, TN
Sample 7	50	WNV/FLAV	~31	~19	Shelby County, TN

**Table 2. The qPCR single-plex and multiplex reaction set-ups**

<b>Single-plex reaction components</b>	<b>Volume per 25 µl reaction</b>	<b>Final concentration</b>
4x TaqMan Fast Virus 1-Step Master Mix	6.25 µl	1x
25 µM Forward primer WNV_1160	0.4 µl	0.4 µM
25 µM Reverse primer WNV_1229c	0.4 µl	0.4 µM
25 µM Probe #1 - FAM (WNV)	0.1 µl	0.1 µM
RNA template (stock)	5 µl	Variable
RT-PCR grade water	9.45 µl	Variable

<b>Multiplex reaction components</b>	<b>Volume per 25 µl reaction</b>	<b>Final concentration</b>
4x One-Step Viral RT-PCR Master Mix	10 µl	1x
100x Multiplex Reverse Transcription Mix	0.4 µl	1x
25 µM Forward primer WNV_1160	0.64 µl	0.4 µM
25 µM Reverse primer WNV_1229c	0.64 µl	0.4 µM
25 µM Forward primer FLD f_16	0.64 µl	0.4 µM
25 µM Reverse primer FLD r_94	0.64 µl	0.4 µM
25 µM Probe #1 - FAM (WNV)	0.32 µl	0.2 µM
25 µM Probe #2 - HEX (FLAV)	0.32 µl	0.2 µM
RNA template (diluted 1:10, 1:100, 1:1,000)	5 µl	Variable
RNase-free water	21.4 µl	Variable

**Table 3. The QIAcuity reverse transcription dPCR reaction set-up for duplex and single-plex reactions**

<b>Single-plex reaction components</b>	<b>Volume per 40 µl reaction</b>	<b>Final concentration</b>
4x One-Step Viral RT-PCR Master Mix	10 µl	1x
100x Multiplex Reverse Transcription Mix	0.4 µl	1x
25 µM Forward primer WNV_1160	0.64 µl	0.4 µM
25 µM Reverse primer WNV_1229c	0.64 µl	0.4 µM
25 µM Probe - FAM (WNV)	0.32 µl	0.2 µM
RNA template (stock and dilutions 1:10 and 1:100)	5 µl	Variable
RNase-free water	23 µl	Variable

<b>Duplex reaction set-up components</b>	<b>Volume per 40 µl reaction</b>	<b>Final concentration</b>
4x One-Step Viral RT-PCR Master Mix	10 µl	1x
100x Multiplex Reverse Transcription Mix	0.4 µl	1x
25 µM Forward primer WNV_1160	0.64 µl	0.4 µM
25 µM Reverse primer WNV_1229c	0.64 µl	0.4 µM
25 µM Forward primer FLD f_16	0.64 µl	0.4 µM
25 µM Reverse primer FLD r_94	0.64 µl	0.4 µM
25 µM Probe #1 - FAM (WNV)	0.32 µl	0.2 µM
25 µM Probe #2 - HEX (FLAV)	0.32 µl	0.2 µM
RNA template (diluted 1:10, 1:100, 1:1,000)	5 µl	Variable
RNase-free water	21.4 µl	Variable



The QIAcuity Nanoplate was then sealed and loaded onto a QIAcuity One, 5plex digital PCR instrument (Cat.No. 911022). Reactions for each of the sample and each of the dilution series were ran in duplicates on the QIAcuity dPCR instrument.

The QIAcuity dPCR workflow consists of three steps as follows: a priming/partitioning of the reactions step, PCR cycling step, and imaging step, which are performed automatically by the instrument. The reverse transcription and PCR amplification of reactions were performed directly in the nanoplate by the QIAcuity One instrument and consisted of a reverse transcription step at 50°C for 40 minutes followed by PCR initial heat activation step at 95°C for 2 minutes followed by 40 cycles of denaturation step at 95°C for 5 seconds and a combined annealing and extension step at 60°C for 30 seconds. The real-time PCR cycling conditions were as follows: a 50°C for 5 minutes step followed by 95°C for 20 seconds step followed by 40 cycles of 95°C for 3 seconds and 60°C for 30 seconds.

The nanoplate was imaged at default imaging settings consisting of a 500 ms exposure and gain 6 for both the green and yellow detection channels. The dPCR analysis

was performed using the QIAcuity Software Suite. A reference dye is included in the master mix, allowing the software to determine which partitions are valid and analyzable. A volume precision factor (VPF) was applied to the quantitation data to account for variations in partition size for different nanoplate batches.

## Results and Discussion

### Single-plex assay

To determine if it was possible to use digital PCR to differentiate between samples with demonstrated low and high  $C_T$  values by qPCR, we selected two samples that had low  $C_T$  values (~20), and two samples that had high  $C_T$  values (<32) to test via dPCR. Using the QIAcuity digital PCR instrument, all four samples were detected and quantified in this study (Table 4). Significantly higher concentrations were observed for samples with low  $C_T$  values (samples 3 and 4) as expected.

Average concentration and positive partition number for sample 3 and 4 were 40.35 copies/ $\mu$ l and 91.2 copies/ $\mu$ l, and 829 positive partitions and

**Table 4. Digital PCR results observed using QIAcuity dPCR system**

qPCR $C_T$ value	Sample	Concentration copies/ $\mu$ l	West Nile Virus		
			CI (95%)	Valid partitions	Positive partitions
High $C_T$	Sample 1 - stock	1.2	40.8%		24
	Sample 1 - stock	0.862	47.4%		18
	Sample 2 - stock	0.192	109.1%	25402	4
	Sample 2 - stock	0.144	130.0%	25434	2
	Sample 1 - 1:10	0.096	168.6%	25459	2
	Sample 1 - 1:10	0.096	168.6%	25447	2
	Sample 2 - 1:10	0.0	–	25428	0
	Sample 2 - 1:10	0.0	274.40%	25411	1
Low $C_T$	Sample 3 - 1:10	39.8	6.80%	25460	818
	Sample 3 - 1:10	40.9	6.70%	25446	840
	Sample 4 - 1:10	89.0	4.50%	25442	1794
	Sample 4 - 1:10	93.4	4.0%	25412	1876
	Sample 3 - 1:100	3.5	22.90%	25454	74
	Sample 3 - 1:100	3.5	22.90%	25433	74
	Sample 4 - 1:100	9.9	13.70%	25405	206
	Sample 4 - 1:100	12.5	12.20%	25420	259
	NTC	0.0	–	25461	0
	Positive control	6083.1	0.60%	24545	24379

1835 positive partitions, respectively for 1:10 dilution series. Whereas average concentration and positive partition number for samples 1 and 2, which were previously shown to produce high  $C_T$  values in qPCR, were 1 copies/ $\mu$ l and 0.12 copies/ $\mu$ l, and 21 positive partitions and 3.5 positive partitions, respectively for stock RNA template.

Consistent results were observed between replicates, which demonstrates that dPCR provides a highly reproducible approach for nucleic acid quantitation. Qualitative analysis of fluorescence intensity showed clear separation between the negative and the positive partition clusters for the single-plex assay with signal-

to-noise ratios of ~6, tight clustering of positive droplets, and no positive partitions observed for the NTC (no template control) (Figure 1).

Interestingly, we were able to detect and quantify sample 1 using QIAcuity, whereas this sample was determined to be negative in qPCR based on amplification curves (Figure 2). This finding supports recent studies demonstrating that dPCR is more accurate and more sensitive compared to the qPCR and is a superior method for low target detection and quantitation. Furthermore, dPCR can be used as a validation method for those samples that were observed as negatives (have high  $C_T$  values) in qPCR analysis.

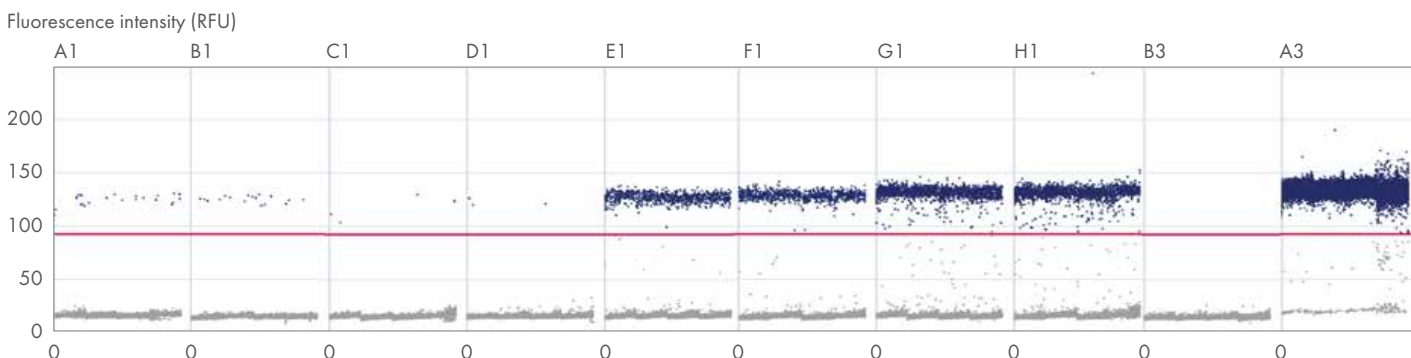


**Figure 1. Clear separation of negative and positive partitions.**

1D plots for WNV target for four samples tested, no template control and a positive control. Stock RNA template was used for samples 1 and 2, whereas 1:10 dilution series were used for samples 3 and 4. All four samples were tested in duplicates.

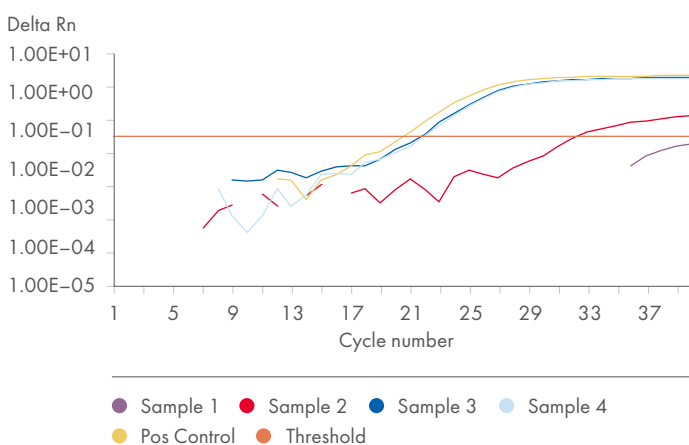


**Figure 2. Low sensitivity of qPCR for Samples 1 and 2.**

qPCR data for the four samples and the corresponding positive control sample that were previously tested on dPCR. Sample 3 and sample 4 represents low  $C_T$  values containing samples, and sample 1 and sample 2 represent high  $C_T$  values containing samples. Threshold shown in orange.

The 2-plex assay was designed to simultaneously detect WNV and FLAV targets, enabling higher through-put sample screening and reducing the cost per target. Using QIAcuity, both WNV and FLAV targets were detected and quantified for all three samples tested (Table 5). On average, 97.3% of a total of 26,000 available partitions were valid and used for concentration calculation across all samples and dilutions. The higher the valid partition number observed, the more precise and accurate the target quantification can be performed which is important when detecting and quantifying low abundant targets.

The 1:10 dilution yielded the highest concentration of WNV target when compared to other dilutions (1:100 and 1:1000) tested. This suggests that the concentration of the WNV target is low for samples tested, and by further diluting RNA template, target molecules become undetectable. The concentration of the FLAV target was higher than WNV, thus copies per microliter were quantified for all three dilutions (Table 5). Sample 5 had the highest concentration (an average of 4.85 copies/ $\mu$ l)

for the WNV target, whereas sample 7 had the lowest (an average of 0.8645 copies/ $\mu$ l). For the FLAV target, sample 6 had the highest concentration (an average of 1940.65 copies/ $\mu$ l), following by sample 7 and sample 5, which showed the lowest (an average of 1410.85 copies/ $\mu$ l and an average of 268.25 copies/ $\mu$ l, respectively) concentrations. When working with multiplex assays, it is important to note that concentrations for different targets within a given sample can be significantly different from one another, thus appropriate dilution of nucleic acid template may need to be performed before analysis. For example, over 78% of total valid partitions generated positive signal for sample 6 diluted 1:10, which is near the upper limit of quantification of the QIAcuity system. Non-diluted stock RNA would have been immeasurable for FLAV in these samples due to the over loading of the dPCR partitions. Positive and negative partition clusters on 1-D scatterplots for all samples and dilution series for both targets are presented in Figure 3.

**Table 5. Concentrations in copies per microliter, confidence interval at 95%, a total number of valid partitions and a total number of positive partitions observed for three samples and dilution series performed for WNV and FLAV**

Sample	West Nile virus (WNV)				Flanders virus (FLAV)			
	Concentration copies/ $\mu$ l	CI (95%)	Valid partitions	Positive partitions	Concentration copies/ $\mu$ l	CI (95%)	Valid partitions	Positive partitions
Sample 5 - 1:10	4.8	19.7%	25215	100	267.8	2.6%	25228	5071
Sample 5 - 1:10	4.9	19.5%	25463	102	268.7	2.7%	25472	4864
Sample 6 - 1:10	3.7	22.6%	25261	76	1947.4	1.0%	24932	19502
Sample 6 - 1:10	3.9	21.9%	25462	81	1933.9	1.0%	25472	19824
Sample 7 - 1:10	0.863	47.4%	25417	18	1401.3	1.2%	25428	16891
Sample 7 - 1:10	0.866	47.4%	25329	18	1420.4	1.2%	25359	16857
Sample 5 - 1:100	0.048	274.40%	25416	1	2.4	28.00%	25450	50
Sample 5 - 1:100	0.0	–	25394	0	2.2	30.20%	25451	43
Sample 6 - 1:100	0.0	–	25384	0	22.4	9.50%	25405	423
Sample 6 - 1:100	0.096	168.60%	25376	2	23.3	9.30%	25417	441
Sample 7 - 1:100	0.191	109.10%	25458	4	152.0	3.70%	25473	2696
Sample 7 - 1:100	0.144	130.0%	25438	3	146.2	4.0%	25443	2581
Sample 5 - 1:1000	0.0	–	25202	0	0.3	79.0%	25197	7
Sample 5 - 1:1000	0.0	–	25178	0	0.2	130.0%	25188	3
Sample 6 - 1:1000	0.0	–	25401	0	1.4	38.40%	25197	27
Sample 6 - 1:1000	0.0	–	25456	0	2.0	31.30%	25188	40
Sample 7 - 1:1000	0.0	–	25302	0	13.1	12.30%	25435	255
Sample 7 - 1:1000	0.0	–	25310	0	10.9	13.40%	25484	215
NTC	0.048	274.40%	25432	1	0.0	–	25441	0
Positive control	443.9	2.10%	23680	7235	1141.0	1.40%	23685	13733

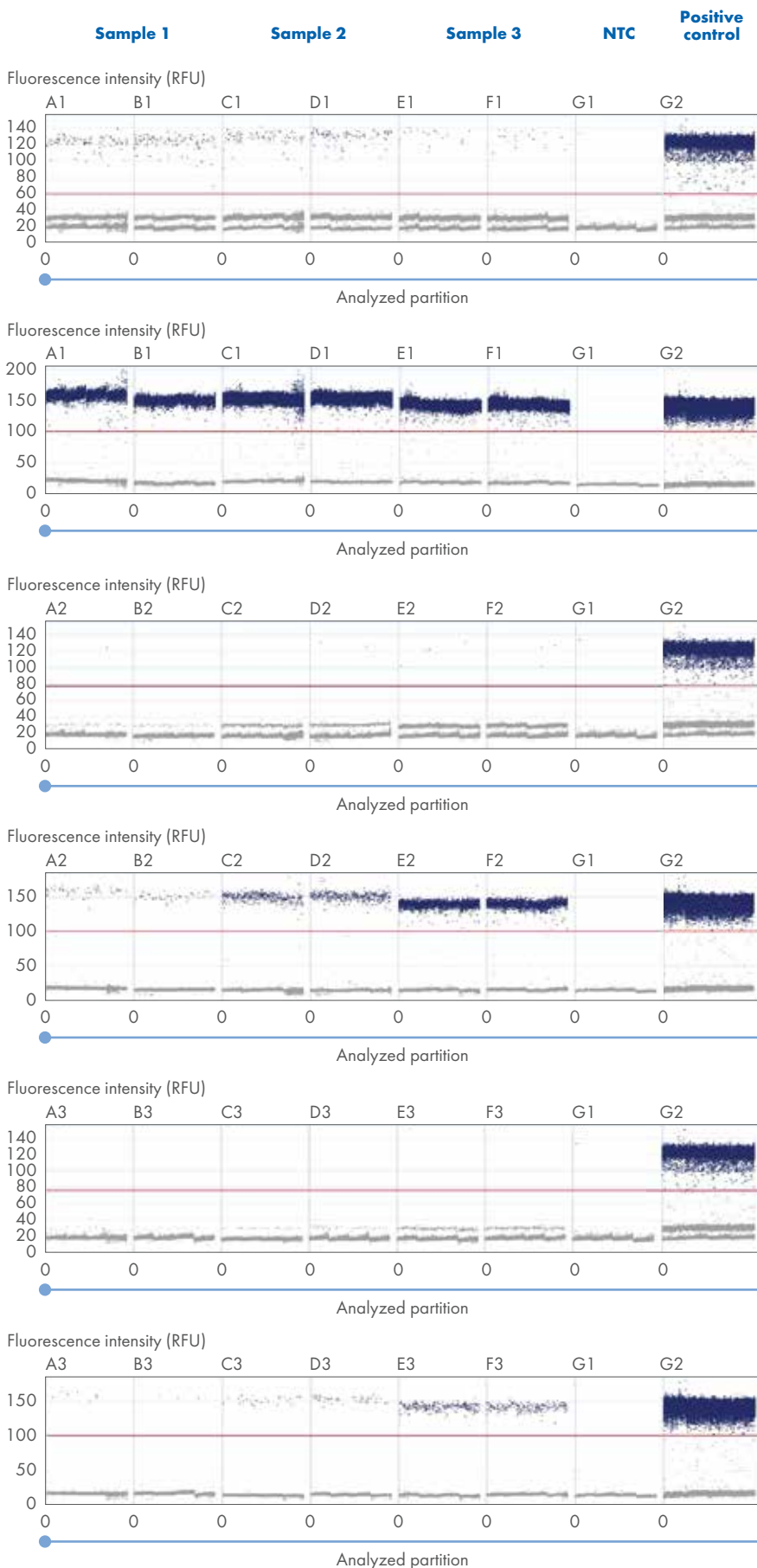


**Figure 3. Multiplex analysis of WNV and FLAV.**

1D plots for WNV and FLAV targets. Red line represents threshold line which separates the positive (dark blue) partition and the negative partition (in grey) clusters. Green detection channel represents WNV target detection and the Yellow detection channel represents FLAV target detection.

- A** WNV target for samples diluted to 1:10;
- B** FLAV target for samples diluted to 1:10;
- C** WNV target for samples diluted to 1:100;
- D** FLAV target for samples diluted to 1:100;
- E** WNV target for samples diluted to 1:1000;
- F** FLAV targets for samples diluted to 1:1000.

Qualitative analysis of fluorescence intensity showed clear separation between the negative and the positive partition clusters (Figure 3). Two negative partition clusters on 1-D scatterplots can be seen for WNV (Figure 3 A, C, E). This can be explained by the bleed-through of the positive partition cluster from the FLAV target (Figure 4). The presence of the second cluster, just slightly higher than the negative partitions clusters becomes minor when FLAV template is more diluted, e.g. 1:1000 dilution series (Figure 3 E).

No false positives were observed in the no-template control (NTC) for the FLAV target. However, a single positive partition was observed for NTC sample for the WNV target. After further investigation of 1D plots, it was determined that signal was likely generated by the presence of an artifact, such as dust, and should be excluded from the analysis.

Overall, high reproducibility and high reliability were observed for replicate samples, which had measured concentrations very close to the concentrations expected based on dilution. Similar results were observed for multiplex qPCR analysis in which FLAV was observed to be at a much higher concentration for the three samples than WNV (Figure 5).

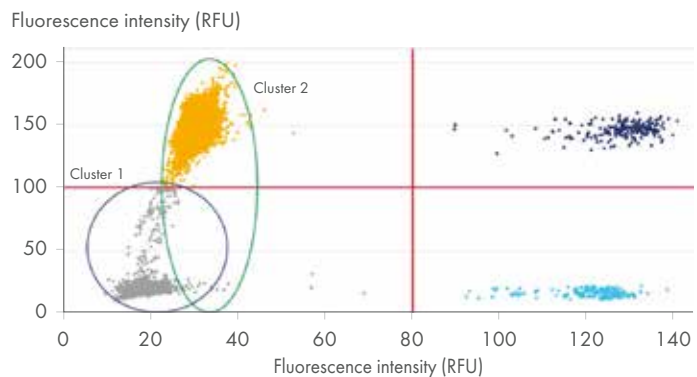


**Figure 4. Multiplex analysis of WNV and FLAV.**

The 2-D scatterplot for the three samples 1:10 dilution series. X-axis represents positive partition cluster for WNV targets. Y-axis represents negative partition cluster in grey and a positive partition cluster for FLAV target in yellow. Dark blue partition cluster represents double positive partitions that contain both target molecules.

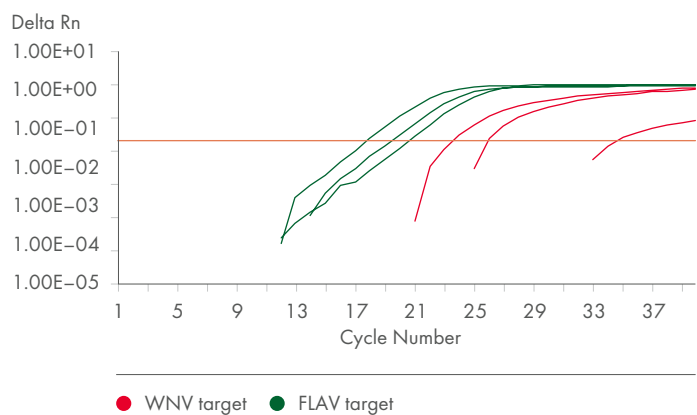


**Figure 5. Multiplex qPCR analysis of WNV and FLAV.**

The qPCR amplification curves for the three samples tested for WNV and FLAV targets. Graph shows detection and quantitation for the WNV target in red, and FLAV target in green. Threshold shown in orange.

## Conclusion

The QIAcuity digital PCR system combined with the QIAcuity One-Step Viral RT-PCR Kit enables precise detection and quantitation of vector-borne viruses in mosquitoes. The results presented in this comparison study showed that digital PCR is a powerful tool for

absolute quantitation of low abundant targets and is a more reliable detection method than qPCR.

Multiplexing allows detection and quantitation of multiple targets in a single reaction more efficiently by increasing sample through-put at a reduced cost per target.

## References

1. Wilson, A.L. et al. (2020) The importance of vector control for the control and elimination of vector-borne diseases. PLOS Neglected Tropical Diseases, 14(1), <https://doi.org/10.1371/journal.pntd.0007831>.
2. Caminade, C. et al. (2019) Impact of recent and future climate change on vector-borne diseases. Ann N Y Aca. Sci. 1436, 157-173.
3. Shaw, W.R. et al. (2019) Vector biology meets disease control: using basic research to fight vector-borne diseases. Nat. Microbiol. 4, 20-34.
4. Lucero, D.E., Carlson T.C., Delisle J., Poindexter S., Jones T.F., and Moncayo A.C. (2016) Spatiotemporal co-occurrence of flanders and West Nile viruses within Culex populations in Shelby County, Tennessee. J. Med. Entomol. 53, 526-532.
5. Lanciotti, R.S. et al. (2000) Rapid detection of west nile virus from human clinical specimens, field-collected mosquitoes, and avian samples by a TaqMan reverse transcriptase-PCR assay. J. Clin. Microbiol. 38, 4066-4071.

## Ordering Information

Product	Contents	Cat. no.
QIAcuity One-Step Viral RT-PCR Kit	4x 1.3 ml One-Step Viral RT-PCR Master Mix (4x), 2x 100 µl Multiplex Reverse Transcription Mix (100x), and 8x 1.9 ml RNase-Free Water	1123145
QIAcuity Nanoplate 26k 24 well	50 QIAcuity Nanoplates 26x 24-well, 55 Nanoplate Seals	250002
QIAcuity Four System	Four-plate digital PCR instrument for detecting up to 5 fluorescent dyes, notebook computer, barcode scanner, roller, USB flash memory and QIAcuity Software Suite: includes installation, training, and 1 preventive maintenance visit, 1 year warranty on labor, travel, and parts	911042

The products mentioned here are intended for molecular biology applications. These products are not intended for the diagnosis, prevention, or treatment of a disease.

For up-to-date licensing information and product-specific disclaimers, see the respective QIAGEN kit handbook or user manual. QIAGEN kit handbooks and user manuals are available at [www.qiagen.com](http://www.qiagen.com) or can be requested from QIAGEN Technical Services or your local distributor.



For more information, visit [www.qiagen.com/dPCR](http://www.qiagen.com/dPCR).

Trademarks: QIAGEN®, Sample to Insight®, QIAcuity®, QIAgility® (QIAGEN Group).

Registered names, trademarks, etc. used in this document, even when not specifically marked as such, may still be protected by law.

© 2022 QIAGEN, all rights reserved. PROM-20283-001 1127182 03/2022